Polyhedron 201 (2021) 115170

Contents lists available at ScienceDirect

Polyhedron

journal homepage: www.elsevier.com/locate/poly

Multi-dimensional copper(I) and silver (I) coordination polymers assembled with a pyridyl *bis*-urea macrocyclic ligand

Bozumeh Som [a,b], Mark D. Smith [b], Linda S. Shimizu [b,*]

[a] Department of Chemistry, University of Ghana, P. O. Box LG 56, Legon, Accra, Ghana
[b] Department of Chemistry and Biochemistry, University of South Carolina, Columbia, SC 29208, United States

ARTICLE INFO

Article history:
Received 2 February 2021
Accepted 18 March 2021
Available online 24 March 2021

Keywords:
Pyridyl bis-urea macrocycle
Self-assembly
Coordination polymer

ABSTRACT

We report the synthesis of a new flexible multimodal macrocyclic ligand, protected pyridyl *bis*-urea macrocycle **1**, and two of its coordination polymers $Cu_2I_2(\mathbf{1})_2{\cdot}(CH_3CN)_{1.63}$ (**2**) and $[Ag(\mathbf{1})](NO_3){\cdot}(H_2O)_{2.49}$ (**3**). The ligand possesses conformational flexibility and adopts different conformations and binding modes depending on the metal ions. The crystal structure of **2** shows a 2D coordination network constructed from rhomboidal Cu_2I_2 dimer units and **1** as a bridging ligand binding through the pyridyl N atoms. **3** forms a sophisticated 3D structure with 1D chains formed by N-Ag-N links between pyridyl N atoms of two adjacent macrocyclic ligands and Ag(I) ions. These chains form 2D layers through longer Ag-O interactions and the chains are linked together into a 3D network by hydrogen bonding involving interstitial water molecules. These results indicate the potential of ligand **1** in the self-assembly of coordination polymers with diverse topology and functional applications.

1. Introduction

The design and synthesis of coordination polymers (CPs) have attracted much attention due to their intriguing topological features and functional properties [1,2]. These complex materials have potential applications for gas storage/separation, [3,4] catalysis, [5] molecular magnetism, [6] and luminescent materials [7,8]. By employing several assembly motifs, scientist have synthesized CPs with emergent properties. For example, the judicious choice of organic ligands and metal ions that have specific directionality gives rise to CPs with diverse solid-state structures (1D, 2D or 3D) and properties [9,10]. Other factors that influence the structural outcome of CPs include temperature, solvents, pH value, and reactants ratio. Each of these factors may influence structural diversity and lead to unpredicted structures [11,12]. In addition to the above-mentioned factors the design of CPs is centered primarily on the ligand type, position of the donor atoms, as well as the length and its flexibility [13]. A suitable metal with a rigid bridging ligand will therefore generate either discrete macrocyclic/cage-like architectures or continuous metal–organic framework materials [9]. On the other hand, bridging ligands with more flexibility give mixtures of coordination polymers due to the lack of control on the outcome of the self-assembly process. Especially in metal–organic frameworks, linear organic polycarboxylates (O-donors) and pyridines (*N*-donors) are among the most used ligands [9,14]. Tuning the flexibility of such ligands can be achieved by introducing groups such as -O-, $-CH_2-$, and -O-CH_2-, enabling free rotation around these groups to fit the coordination geometry of the metal ions in the assembly process.

The Shimizu research group has demonstrated the use of pyridyl/bipyridyl urea macrocycles in the synthesis of coordination complexes in previous reports [15,16]. These functionalized macrocycles showed remarkable flexibility where the macrocycle can rotate to access different binding conformations in which metal ions could be in the interior of the macrocycle (*endo*) or on its exterior (*exo*) [15–17]. The protected pyridyl/bipyridyl urea macrocycles have displayed diverse coordination modes with alkali and transition metal ions using both oxygen and nitrogen donor atoms. Our primary task in the current study was to investigate the flexibility and coordination modes of macrocyclic ligand **1** that was anticipated to bind metal ion(s) through the exterior pyridyl nitrogen(s). Herein, we report the syntheses and characterization of this new pyridyl bis-urea macrocycle **1** and, its Cu(I) and Ag(I) coordination complexes where the pyridyl Ns are key in determining the architecture of the CPs (Fig. 1).

* Corresponding author.
E-mail address: deposite@ccdc.cam.ac.uk (L.S. Shimizu).

https://doi.org/10.1016/j.poly.2021.115170
0277-5387/

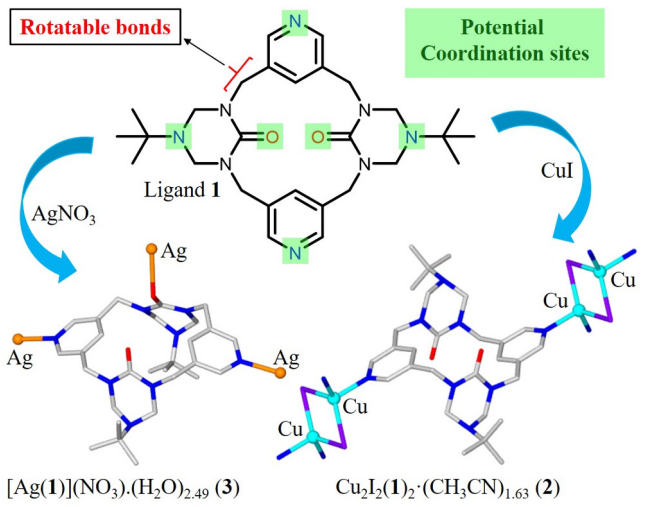

Fig. 1. Schematic structure of flexible macrocyclic ligand **1** used for the synthesis of CPs.

2. Experimental

Materials and methods. Unless otherwise specified, all chemicals were purchased from commercial sources (Sigma-Aldrich, Alfa Aesar, TCI or VWR) and used without further purification. Dimethyl pyridine-3,5-dicarboxylate, 3,5-bis(hydroxymethyl)pyridine and 3,5-bis(bromomethyl)pyridine hydrobromide were prepared according to published literature procedures respectively [18–20]. Triazinanone was prepared as previously described [21]. ^{1}H NMR and ^{13}C NMR were recorded on Varian Mercury/VX 400 NMR spectrometer. FT-IR spectra were obtained with a Perkin Elmer Spectrum 100 FT-IR Spectrometer over the range 4000–650 cm^{-1} with 2 cm^{-1} resolution and 32 scans per sample.

3. Ligand synthesis

Dimethyl pyridine-3,5-dicarboxylate. Thionyl chloride (1.3 mL, 17.94 mmol) was added dropwise to a stirring solution of pyridine-3,5-dicarboxylic acid (1.0 g, 5.98 mmol) in dry methanol (10 mL) at 0 °C. The reaction was heated at reflux (3 h) after which the mixture was cooled to room temperature then concentrated *in vacuo*. The residue was diluted with water (100 mL) and extracted with ethyl acetate (100 mL). The aqueous layer was neutralized with 8 M NaOH solution and extracted with ethyl acetate again (100 mL). The combined organic layers were washed with saturated $NaHCO_3$ solution and brine, dried over anhydrous Na_2SO_4. Finally, the solvent was removed under reduced pressure to give a white solid material (0.8 g, 68% yield).^{1}H NMR (300 MHz, $CDCl_3$): δ = 9.37 (d, J = 2.0 Hz, 2H), 8.87 (t, J = 2.1 Hz, 1H), 3.99 (s, 6H).

3,5-Bis(hydroxymethyl)pyridine. Dimethyl pyridine-3,5-dicarboxylate (2.10 g, 10.76 mmol) was dissolved in dry THF (150 mL) and added dropwise to a suspension of $LiAlH_4$ (1.02 g, 26.90 mmol in 150 mL of THF) in an ice/acetone bath (0 ℃) under nitrogen. After addition, the resulting yellow mixture could warm gradually to r.t. then left stirring overnight. Upon completion, the reaction mixture was quenched by sequentially adding H_2O (1 mL), 10% NaOH (2 mL) and H_2O (3 mL). The mixture was suction filtered, and the yellow filtrate dried over anhydrous $MgSO_4$. Removal of the solvent under reduced pressure followed by drying under vacuum gave a yellow solid crude (1.12 g, 75% yield). The product was used directly for the next reaction without any further purification.

3,5-Bis(bromomethyl)pyridine Hydrobromide. The crude 3,5-bis (hydroxymethyl)pyridine (1.12 g, 8.05 mmol) was added to a 250 mL round bottom flask and 48% HBr (15 mL) was added slowly and carefully. The reaction mixture was stirred and heated at 125 ℃ for 6 h. The reaction mixture was cooled to room temperature, and 40 mL H_2O added slowly then adjusted the pH to 8 with saturated $NaHCO_3$. The resulting whitish precipitate was collected by suction filtration and washed with H_2O (10 mL). This crude product was dried under vacuum overnight (1.56 g, 55.86% yield). ^{1}H NMR (300 MHz, $CDCl_3$): δ = 8.56 (d, J = 2.0 Hz, 2H), 7.77 (t, J = 2.0 Hz, 1H), 4.47 (s, 4H).

*Macrocyclic ligand, **1**.* An oven dried 500 mL round bottom flask was filled with a suspension of triazinanone (0.30 g, 1.88 mmol) and NaH (0.39 g, 9.76 mmol) in dry THF (100 mL) and refluxed for 2 h under nitrogen then cooled to room temperature. To this cooled mixture a solution of 3,5-*bis*(bromomethyl)pyridine hydrobromide (0.65 g, 1.88 mmol) in THF (50 mL) was added in one portion (Scheme 1). The reaction mixture stirred and heated to reflux under nitrogen for 48 h while monitoring the reaction with silica gel TLC. Upon completion (based on TLC monitoring), the reaction mixture was cooled to room temperature and quenched with water (100 mL). The volume of the resulting solution was reduced by rotary evaporation to a minimum and extracted with dichloromethane (DCM) (3 × 100 mL). The DCM layers were combined, washed with brine, dried over anhydrous $MgSO_4$ and the solvent removed under reduced pressure to give a yellow solid. Purification of the crude material (wet loaded) by silica gel chromatography with $CHCl_3$/MeOH (9:1) afforded macrocyclic ligand **1** as a dimer (0.15 g, 30.64%). X-ray quality single crystals of this macrocycle were grown by slow evaporation from toluene (3 mg / 1 mL). Macrocyclic ligand **1**; ^{1}H NMR (400 MHz, TCE) δ 8.40 (s, 2H), 7.98 (s, 1H), 4.64 (s, 4H), 4.26 (s, 4H), 1.14 (s, 9H).; ^{13}C NMR (101 MHz, CD_3CN) δ = 156.58, 148.67, 135.86, 62.92, 54.78, 46.16, 28.50: Melting point 268–271 ℃. HRMS (ES) calculated for $C_{28}H_{40}N_8O_2$: [M + H], 521.3347. Observed m/z 521.3351. IR (neat ATR) 2969, 1630, 1503, 1427, 1362, 1302, 1202, 1156, 1025, 955, 893, 793, 752, 707 cm^{-1}.

Coordination polymer $Cu_2I_2(1)_2\cdot(CH_3CN)_{1.63}$, (2). The protected pyridyl macrocyclic ligand **1** (10 mg, 0.0192 mmol) was dissolved in DCM (1 mL) and was added to an acetonitrile solution of CuI (3.65 mg, 0.0192 mmol in 1.0 mL). The mixture was then stirred at room temperature for an hour. This resulted in a white powder that was collected by filtration, washed with diethyl ether-acetonitrile mixture and chloroform then dried under vacuum. Yield: 10.4 mg (76%). X-ray quality single crystals were grown by dissolving 3 mg of the powder obtained from the above synthesis

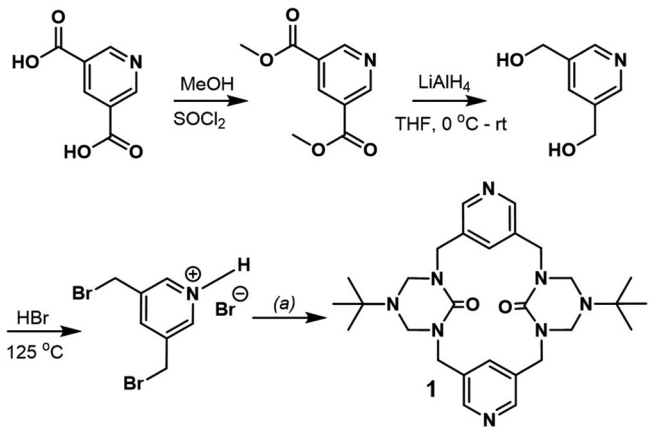

Scheme 1. Synthesis of pyridyl *bis*-urea macrocyclic ligand **1** [a]Reagents and conditions: (a) triazinanone (in THF), NaH, refluxed for 1 h, cooling, followed by addition of 3,5-*bis*(bromomethyl)pyridine hydrobromide in THF, then refluxed for 48 h.

in 10 mL acetonitrile and allowed to slowly evaporate over 5 days. IR (neat ATR): 3479, 2973, 1638, 1511, 1436, 1366, 1304, 1234, 1197, 1143, 1029, 959, 894, 795,752, 703 cm^{-1}.

Coordination polymer [Ag(1)](NO$_3$)·(H$_2$O)$_{2.49}$, (3). Ligand **1** (3.0 mg, 5.76 × 10^{-3} mmol) and $AgNO_3$ (1.95 mg, 11.5 × 10^{-3} mmol) were each dissolved in hot acetonitrile (1.0 mL). The solutions were mixed thoroughly and filtered through a Millipore filter, cooled, and allowed to slowly evaporate over 2–3 days. A cluster of colorless block crystals formed that were suitable for single crystal X-ray diffraction. Yield was 70% (2.96 mg). IR (neat ATR): 3409, 2969, 1632, 1513,1420, 1304,1199, 1156, 1031, 960, 932, 900, 796, 757, 701 cm^{-1}.

X-ray Crystal Structure Determination. Diffraction data of ligand **1** and the coordination polymers (**2** and **3**) were collected at 100(2) K using a Bruker D8 QUEST diffractometer equipped with a PHOTON-100 CMOS area detector and an Incoatec microfocus source (Mo Kα radiation, λ = 0.71073 Å). The raw area detector data frames were reduced and corrected for absorption effects using the Bruker APEX3, SAINT + and SADABS programs [22,23]. Final unit cell parameters were determined by least-squares refinement of large sets of reflections taken from the data sets. All structures were solved with SHELXT [24,25]. Subsequent difference Fourier calculations and full-matrix least-squares refinement against F^2 were performed with SHELXL-2017 [24,25] using OLEX2 [26]. A summary of the crystallographic data and structure refinements are given here in Table 1 and further details in the supporting information.

4. Results AND DISCUSSION

Ligand Design and Synthesis. The new pyridyl *bis*-urea macrocyclic ligand (**1**) was synthesized following a previously reported procedure [27] to give a yield of 30.6%. The proton NMR of **1** was first recorded at room temperature in chloroform-*d* then in acetonitrile d_3(Fig. S1). However, in both cases we were missing the peak associated with the methylene group in between the pyridyl rings and the protected urea groups. In both spectra of **1**, the sixteen methylene protons are broad signals at δ 4.22 ppm in chloroform-*d* and 4.20 ppm in acetonitrile d_3. The broadening and only one signal observed for these sixteen methylene protons in the room temperature ^{1}H NMR suggest the presence of two or more conformations slowly interconverting on the NMR time scale. So, we turned to high temperature ^{1}H NMR (variable temperature NMR) to observe the chemical shift of these methylene groups. Upon running the experiment in a high boiling NMR solvent (1,1,2,2-Tetrachloroethane-d_2) at higher temperature (125 ℃) two sets of signals were obtained (at δ = 4.64 ppm and 4.26 ppm) for these sixteen methylene protons (Fig. S2). Integration of these peaks gave a ratio of 1:1 representing eight benzylic protons (δ = 4.64 ppm) and eight protons from the heterocyclic ring methylene groups (δ = 4.26 ppm). The ^{13}C NMR spectrum of macrocycle **1** exhibits the requisite number of signals at both room temperature and high temperature (125 ℃). Fig. S3 shows ^{13}C NMR spectrum of macrocycle **1** in acetonitrile d_3 at room temperature. X-ray quality single crystals **1** were crystallized from toluene (3 mg / 1 mL) by slow evaporation to give good solvent-free colorless rhombic plates. The macrocycle (**1**) crystallizes in the triclinic space group *P*-1 (No. 2) as confirmed by structure solution. The asymmetric unit consists of one complete macrocyclic ligand **1** molecule and half each of two additional ligand **1** molecules, both of which are located on crystallographic inversion centers. There are three crystallographically independent molecules, two of which are centrosymmetric (Fig. 2). All the three molecules of **1** adopted the 1,2-alternate conformation in the crystal structure. The pyridyl N atoms in the structure are poised on the exterior and pointing in opposite directions whilst the urea carbonyl groups and triazinanone rings are antiparallel to each other. Packing structure of **1** in the solid state revealed that the molecules are layered on top each other. There are two layers; one made of molecule A and the other made of alternating molecule B and molecule C (Fig. 3).

Macrocyclic ligand **1** and its constitutional isomer (**4**) [27] as depicted in Fig. 4, can be considered as analogues of calix[4]arenes, which are of special interest due to their ability to adopt well-defined three-dimensional structures. Calix[4]arenes are commonly discussed in terms of four basic conformations: cone, partial cone, 1,2- and 1,3-alternate [28,29]. Prior reports of pyridyl bis-urea macrocycle **4** showed that it adopted two conformations in

Table 1
Crystallographic data and structure refinement parameters of macrocyclic ligand **1**, and Cu_2I_2(**1**)$_2$·$(CH_3CN)_{1.63}$ (**2**) and [Ag(**1**)](NO_3).$(H_2O)_{2.49}$ (**3**).

	1	Cu_2I_2(1)$_2$·$(CH_3CN)_{1.63}$ (2)	[Ag(1)](NO_3).$(H_2O)_{2.49}$ (3)
Empirical formula	$C_{28}H_{40}N_8O_2$	$C_{59.26}H_{84.89}Cu_2I_2N_{17.63}O_4$	$C_{28}H_{44.98}AgN_9O_{4.49}$
Formula weight	520.68	1489.15	735.42
T/K	100(2)	100(2)	100(2)
Crystal system	triclinic	triclinic	triclinic
Space group	*P*-1	*P*-1	*P*1
a/Å	10.6246(5)	8.6693(4)	8.9880(3)
b/Å	11.0831(5)	13.1139(7)	9.1999(3)
c/Å	22.5999(11)	15.1067(8)	10.5400(4)
α/°	90.020(2)	96.502(2)	70.9060(10)
β/°	90.197(2)	97.650(2)	88.585(2)
γ/°	94.120(2)	93.897(2)	76.0530(10)
Volume/Å^3	2654.3(2)	1685.20(15)	797.92(5)
Z	4	1	1
ρ_{calc}g/cm^3	1.303	1.467	1.530
μ/mm^{-1}	0.086	1.604	0.693
F(000)	1120.0	760.0	383.0
Crystal size/mm^3	0.26 × 0.2 × 0.18	0.2 × 0.14 × 0.04	0.16 × 0.1 × 0.04
2θ range/°	5.13 to 60.344	4.414 to 58.256	4.678 to 60.342
Reflections collected	146,413	66,300	48,759
Independent reflections	15,682 [R_{int} = 0.0483, R_{sigma} = 0.0352]	9060 [R_{int} = 0.0433, R_{sigma} = 0.0324]	9401 [R_{int} = 0.0344, R_{sigma} = 0.0319]
Data/restraints	15682/0	9060/200	9401/107
Parameters	699	491	489
GoF on F^2	1.036	1.060	1.037
Final R indexes [I>=2σ (I)]	R_1 = 0.0449, wR_2 = 0.1090	R_1 = 0.0344, wR_2 = 0.0703	R_1 = 0.0276, wR_2 = 0.0509
Final R indexes [all data]	R_1 = 0.0635, wR_2 = 0.1183	R_1 = 0.0524, wR_2 = 0.0773	R_1 = 0.0329, wR_2 = 0.0525
$\Delta\rho_{max./min.}$ (e Å^{-3})	0.42/−0.24	1.04/−0.73	0.32/−0.38

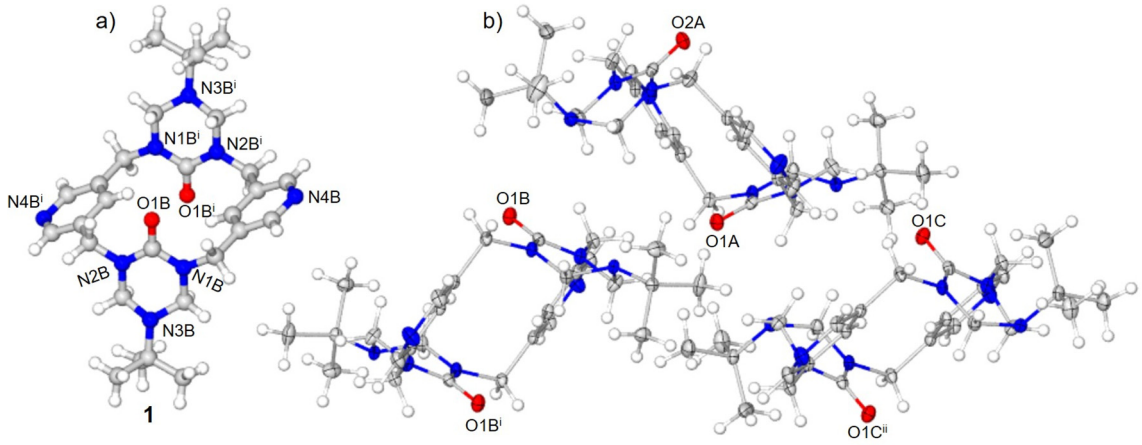

Fig. 2. Components of the structure of macrocyclic ligand **1**. a) Structure of component B. b) Three crystallographically independent, chemically similar molecules. Molecules B and C are located on crystallographic inversion centers. Superscripts denote symmetry-equivalent atoms. Displacement ellipsoids drawn at the 60% probability level.

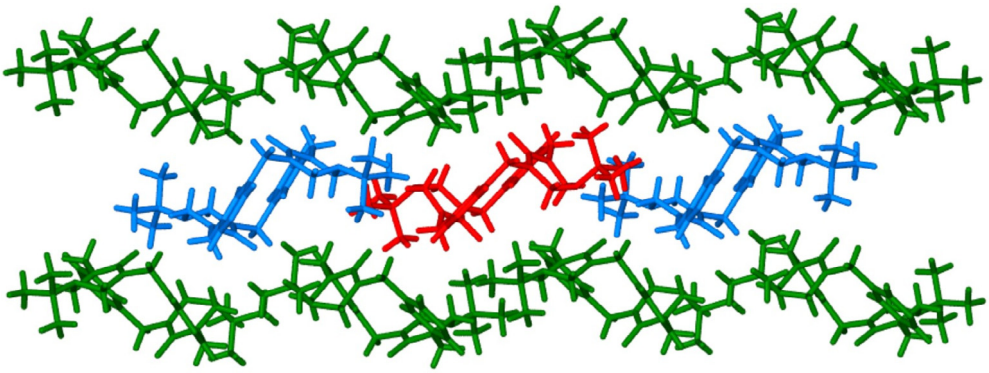

Fig. 3. Packing diagram of ligand **1**. Layered structure made of two types of layers. Layer 1 (top and bottom) is made of only molecule A, and layer 2 (middle) is made of alternating molecule B and C. Color coded for the crystallographically independent, chemically similar molecules. Molecules A (green), B (blue) and C (red).

the solid state, a partial cone and 1,3-alternate when crystalized from two different solvents, *o*-xylene and DMSO respectively [27]. In comparison ligand **1** adopted the 1,2-alternate when crystallized from toluene. This suggests that the solvent of crystallization has a greater influence on the conformation adopted by these macrocycles. Elucidation of the solid-state crystal structures of the two macrocyclic isomers (**1** and **4**) shows more access to the heteroatom binding sites (potential oxygen and pyridine binding sites) in **1** than **4**. This is particularly important for crystal engineering of coordination polymers, as it will lead to the production of multi-dimensional molecular architectures which is of significance in the quest for new functional materials [30].

Crystal structure of $Cu_2I_2(\mathbf{1})_2{\cdot}(CH_3CN)_{1.63}$ (2). Coordination polymer $Cu_2I_2(\mathbf{1})_2{\cdot}(CH_3CN)_{1.63}$ (**2**) crystallizes in a triclinic space group *P*-1 (No. 2). The asymmetric unit consists of one Cu and one I atom, half each of two (**1**) ligands and two acetonitrile molecules (Fig. 5). There are two crystallographically independent macrocyclic ligands. One of the macrocyclic ligands is disordered across an inversion center over two orientations and there is some acetonitrile mixed among the disordered ligand atoms. Only the protected urea part is disordered; the CH_2(pyridyl)CH_2 linker is common to both. The disorder components each have an occupancy of 50%. The single crystal X-ray diffraction analysis reveals that $Cu_2I_2(\mathbf{1})_2{\cdot}(CH_3CN)_{1.63}$ (**2**) is a 2D sheet coordination polymer where the macrocyclic ligands link Cu_2I_2 units through pyridyl N atoms into infinite 2D layers parallel to the crystallographic (1–1–1) plane (Fig. 6). The Cu_2I_2 group forms a rhombus. Each Cu(I) center is further coordinated by two pyridyl N atoms of the ligands creating a tetrahedral coordination geometry around the Cu(I) center (d(Cu–N) = 2.070(2) Å (Cu1-N4) and 2.074(2) Å (Cu1-N8)). Cu-I bond lengths are 2.6051(4) and 2.6294(4) Å. The Cu····Cu distance is 2.5989(6) Å as a diagonal of the Cu_2I_2 rhombus repeating motif. This Cu····Cu distance is shorter than the sum of the van der Waals radii of two Cu atoms (2.80 Å) [31] and remarkably close to that in copper metal (2.56 Å), suggesting strong cuprophillic interaction that may significantly affect the photophysical properties [32,33]. In this structure, ligand **1** acted as a bidentate-bridging ligand coordinating the Cu(I) centers with both pyridyl N atoms.

Crystal structure of $[Ag(\mathbf{1})](NO_3).(H_2O)_{2.49}$ (3). The crystal structure of $[Ag(\mathbf{1})](NO_3).(H_2O)_{2.49}$ (**3**) was confirmed by single crystal X-ray diffraction. It crystallizes in the triclinic system with the acentric group *P*1 (No. 1). Structural analysis revealed that the Ag(I) center adopts a distorted tetrahedral coordination geometry, bonded to two pyridyl N donors, one carbonyl O donor from ligand **1**, and the O atom of a nitrate anion (Fig. 7). In this structure the macrocyclic ligand **1** adopted a flattened cone conformation with the carbonyl groups on the same side. The Ag-N bond distances were 2.167(2) and 2.166(2) Å, while the Ag-O bond distances are 2.517(2) and 2.529(14) Å. There are 1D chains formed by N-Ag-N links (angle 154°) between pyridyl N atoms of two adjacent macrocyclic ligands and the Ag(I) ion (Fig. 8). A further Ag-O interaction of 2.517(2) Å links the Ag centers to a carbonyl oxygen atom O2 of neighboring chain, forming 2D layers (Fig. 9). Furthermore, OH-N hydrogen bonding between the interstitial water molecules and a

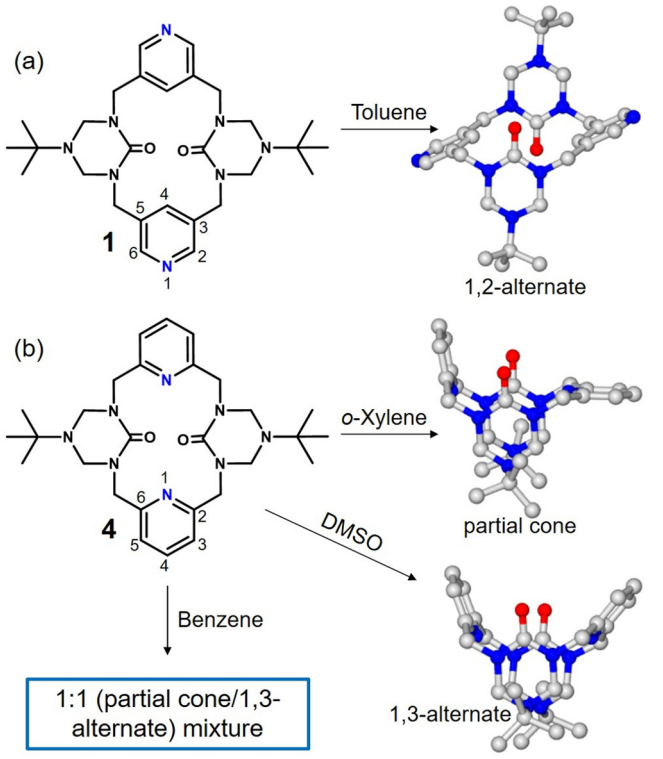

Fig. 4. Comparison of the triazinanone protected pyridyl *bis*-urea macrocycles **1** and **4**. (a) Macrocycle **1** adopted a 1,2-alternate conformation when crystallized from toluene. (b) Comparison of conformers of **4** obtained under three crystallization conditions: (i) partial cone conformation from *o*-xylene, (ii) 1,3-alternate conformation from DMSO and (iii) A 1:1 mixture of partial cone/1,3-alternate conformations from benzene.[27] Hydrogen atoms in crystal structures are omitted for clarity.

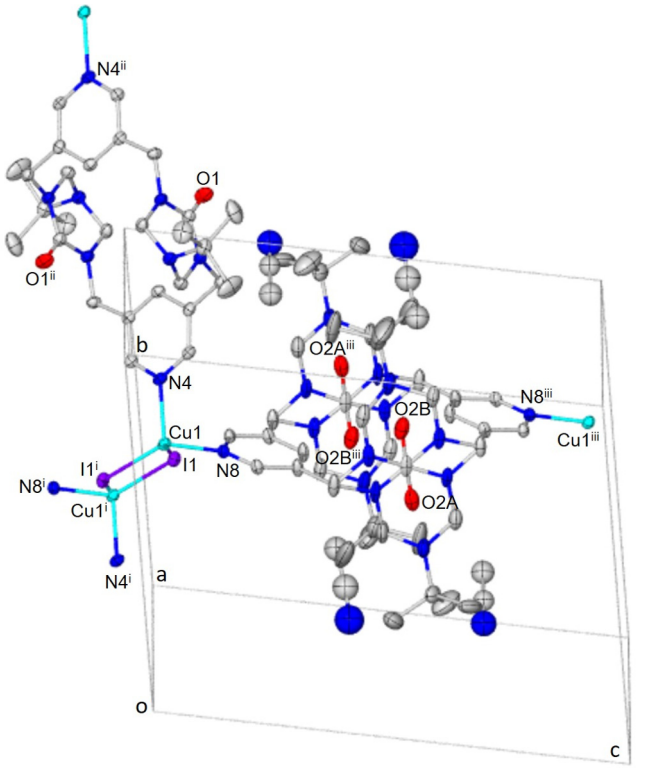

Fig. 5. Components of the crystal structure of $Cu_2I_2(\mathbf{1})_2{\cdot}(CH_3CN)_{1.63}$ (**2**) expanded by symmetry. One ligand is disordered about a crystallographic inversion center along with acetonitrile. Displacement ellipsoids drawn at the 50% probability level. Superscripts denote symmetry-equivalent atoms.

protecting group N atom forms a 3D structure. The nitrate anions are located near Ag but are disordered over three sites (Ag1-O3A/B/C ranging from 2.53 to 2.65 Å). The interstitial water molecules are disordered but occupy closely separated split sites, allowing for location of their hydrogen atoms.

FT-IR spectroscopy. Further investigation on different functionalities present in the ligand structure and the change in electronic states upon complexation are analyzed using FT-IR. Comparison of the solid-state infrared (IR) spectra of the synthesized ligand **1** and coordination polymers is shown in (Fig. 10). The results were consistent with the single crystal X-ray diffraction structural results in terms of the key dominant vibrational modes of the coordinated ligand observed in the 650–4000 cm^{-1} range. The IR spectrum of ligand **1** exhibited a strong band at 1631 cm^{-1} which is attributed to the carbonyl (C═O) group. Upon coordination the intensity of this band decreased in both $Cu_2I_2(\mathbf{1})_2{\cdot}(CH_3CN)_{1.63}$ (**2**) and $[Ag(\mathbf{1})](NO_3).(H_2O)_{2.49}$ (**3**). In coordination polymer $Cu_2I_2(\mathbf{1})_2{\cdot}(CH_3CN)_{1.63}$ (**2**) the band is split in two at 1615 and 1638 cm^{-1}, indicating two different carbonyl groups are present in the complex. This agrees with the single crystal X-ray structure of $Cu_2I_2(\mathbf{1})_2{\cdot}(CH_3CN)_{1.63}$ (**2**) which displays two crystallographically independent macrocyclic ligands of **1**. A similar splitting of the carbonyl group was observed in the spectrum of $[Ag(\mathbf{1})](NO_3).(H_2O)_{2.49}$ (**3**) at 1615 and 1632 cm^{-1} corresponding to a coordinating carbonyl group (C═O-Ag) and an uncoordinated carbonyl group (C═O) respectively. Another key functional group in the structure of ligand **1** is the C═N (pyridine) group. The absorption band of this group has shifted to higher wavenumbers (by 7–10 cm^{-1}) in the coordination polymers. Broad bands are observed at 3479 cm^{-1} for $Cu_2I_2(\mathbf{1})_2{\cdot}(CH_3CN)_{1.63}$ (**2**) and 3409 cm^{-1} for $[Ag(\mathbf{1})](NO_3)$.

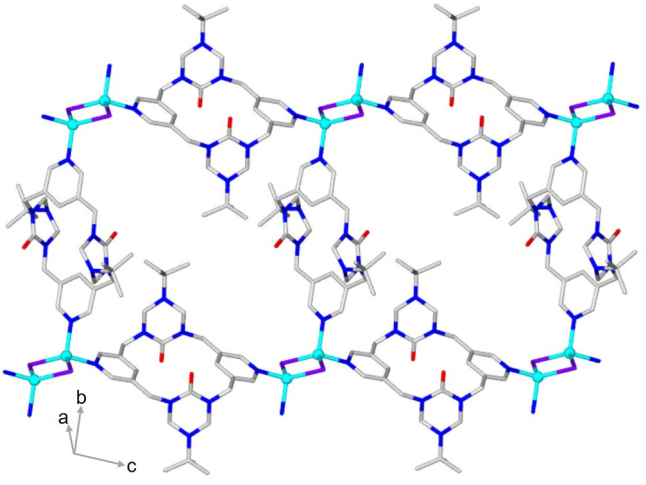

Fig. 6. Coordination network of $Cu_2I_2(\mathbf{1})_2{\cdot}(CH_3CN)_{1.63}$ (**2**) with disorder component B. Macrocyclic ligands link Cu_2I_2 units through pyridyl N atoms into infinite 2D layers. Solvent molecules are omitted for clarity.

$(H_2O)_{2.49}$ (**3**), which are absent in the spectrum of ligand **1**. These bands are attributed to the interstitial solvent molecules (CH_3CN and H_2O) present in the structures of $Cu_2I_2(\mathbf{1})_2{\cdot}(CH_3CN)_{1.63}$ (**2**) and $[Ag(\mathbf{1})](NO_3).(H_2O)_{2.49}$ (**3**) respectively.

5. Conclusion

In summary, the redesigned pyridyl bis-urea macrocyclic ligand (**1**) showed several structural differences when compared to its

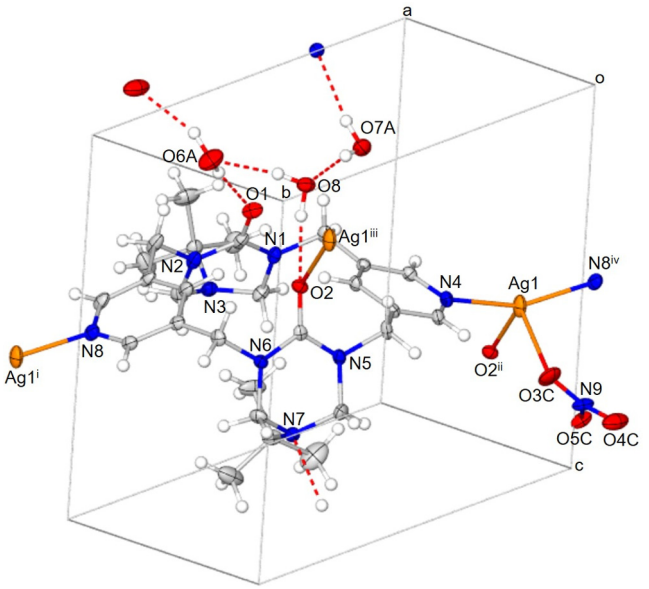

Fig. 7. Components of the crystal structure of $[Ag(\mathbf{1})](NO_3).(H_2O)_{2.49}$ (**3**). Asymmetric unit of the crystal structure of **3** with additional atoms to complete Ag and ligand coordination environments. Only one component each of the disordered nitrate and water molecules are shown. Hydrogen bonds are dashed lines. Displacement ellipsoids drawn at the 50% probability level. Superscripts denote symmetry-equivalent atoms.

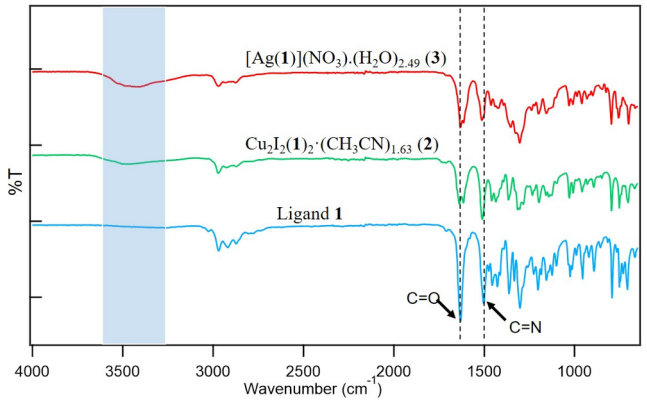

Fig. 10. FT-IR profiles of ligand **1** and coordination polymers (**2**–**3**) in the range 4000–650 cm^{-1}.

ligand **1** adopted the 1,2-alternate conformation when crystallized from toluene, while **4** adopted the partial cone and the 1,3-alternate conformations when crystallized from *o*-xylene and DMSO, respectively. Two coordination polymers $Cu_2I_2(\mathbf{1})_2{\cdot}(CH_3CN)_{1.63}$ (**2**) and $[Ag(\mathbf{1})](NO_3).(H_2O)_{2.49}$ (**3**), have been synthesized by reacting macrocyclic ligand **1** with copper(I) iodide and silver(I) nitrate, respectively. Structural characterization shows that ligand **1** is flexible and can adopt different coordination modes with different

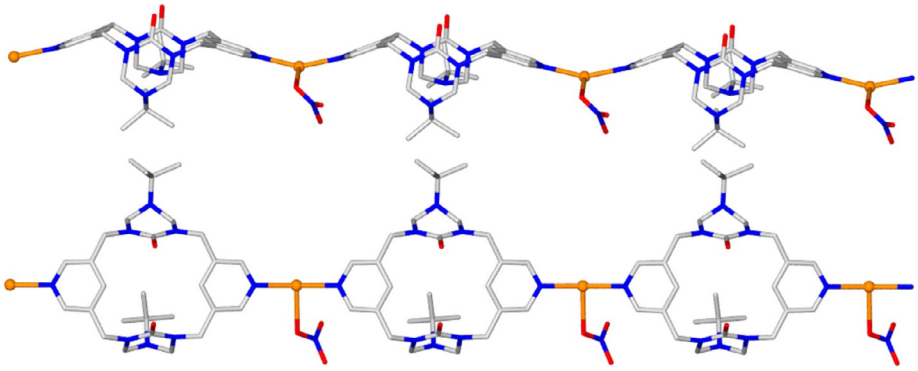

Fig. 8. 1D chains showing the side and top views of the coordination environments of $[Ag(\mathbf{1})](NO_3).(H_2O)_{2.49}$ (**3**) along the crystallographic [1 1 0] direction. One nitrate disorder component shown. Solvent molecules and hydrogens are omitted for clarity.

previously reported positional isomer (**4**)[27]. These dimers (**1** and **4**) adopted different conformations in the solid state. Macrocyclic metal ions. In $Cu_2I_2(\mathbf{1})_2{\cdot}(CH_3CN)_{1.63}$ (**2**), ligand **1** is a bidentate ligand only binding through the pyridyl N atoms. However, ligand

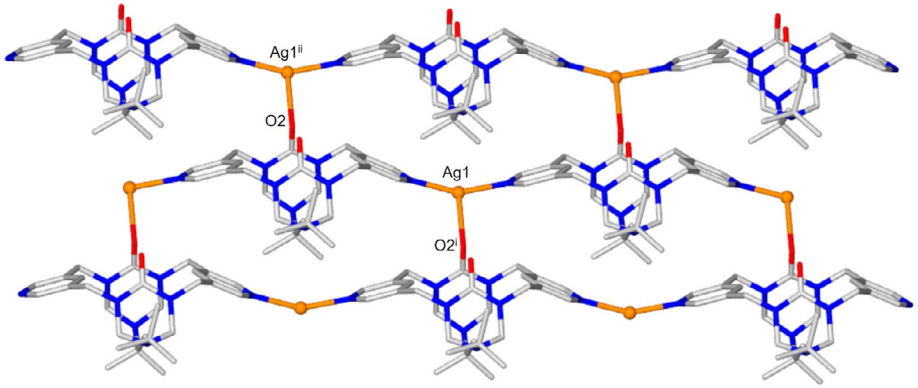

Fig. 9. 2D layers in crystal structure of $[Ag(\mathbf{1})](NO_3).(H_2O)_{2.49}$ (**3**). Ag1-O2 interaction between chains creates 2D layers parallel to the crystallographic (0 0 1) plane. Solvent molecules and nitrate ions are omitted for clarity.

1 behaved as a tridentate ligand in $[Ag(\mathbf{1})](NO_3).(H_2O)_{2.49}$ (**3**), binding through the pyridyl N atoms and one carbonyl O atom. These coordination polymers present extended architectures with interesting dimensionality from 1D to 3D structures. While uncommon, the coordination complexes characterized do exhibit partial solvent occupancy. Current studies probe the effects of solvent and crystallization conditions to evaluate if additional crystal forms with different geometries are readily accessible. Based on these results, further syntheses, and studies of ligand **1** complexes of Cu(I) and Ag(I) containing different anions to determine if that is a structural determinant or has any influence on the luminescence properties of the complexes.

Synopsis

A new multimodal flexible pyridyl *bis*-urea macrocyclic ligand and its Cu(I) and Ag(I) coordination polymers have been synthesized and structurally characterized by single crystal X-ray diffraction. The coordination polymers displayed extended architectures with interesting dimensionality from 1D to 3D structures.

Declaration of Competing Interest

The Authors declare that they have no known competing financial interests of personal relationships that could have appeared to influence the work reported in this paper.

Appendix A. Supplementary data

CCDC <2060221-2060223> contains the supplementary crystallographic data for <**1**-**3**>. These data can be obtained free of charge via http://www.ccdc.cam.ac.uk/conts/retrieving.html, or from the Cambridge Crystallographic Data Centre, 12 Union Road, Cambridge CB2 1eZ, UK; fax: (+44) 1223-336-033; or email: deposite@ccdc.cam.ac.uk. Supplementary date to this article can be found online at http://doi.org/10.1016/j.poly.2021.#. Supplementary data to this article can be found online at https://doi.org/10.1016/j.poly.2021.115170.

References

[1] W.L. Leong, J.J. Vittal, Chem. Rev. 111 (2011) 688–764.
[2] L. Carlucci, G. Ciani, D.M. Proserpio, T.G. Mitina, V.A. Blatov, Chem. Rev. 114 (2014) 7557–7580.
[3] O.K. Farha, A. Özgür Yazaydın, I. Eryazici, C.D. Malliakas, B.G. Hauser, M.G. Kanatzidis, S.T. Nguyen, R.Q. Snurr, J.T. Hupp, Nature Chemistry, 2 (2010) 944
[4] S. Ma, H.-C. Zhou, Chem. Commun. 46 (2010) 44–53.
[5] M. Zhao, S. Ou, C.-D. Wu, Acc. Chem. Res. 47 (2014) 1199–1207.
[6] P. Dechambenoit, J.R. Long, Chem. Soc. Rev. 40 (2011) 3249–3265.
[7] N. Nuñez-Dallos, N. Lopez-Barbosa, A. Muñoz-Castro, D. Mac-Leod Carey, A. De Nisi, M. Monari, J.F. Osma, J. Hurtado, J. Coord. Chem., 70 (2017) 3363-3378
[8] S.W. Jaros, J. Sokolnicki, A. Woloszyn, M. Haukka, A.M. Kirillov, P. Smolenski, J. Mater. Chem. C 6 (2018) 1670–1678.
[9] S.-L. Wang, F.-L. Hu, J.-Y. Zhou, Y. Zhou, Q. Huang, J.-P. Lang, Cryst. Growth & Des. 15 (2015) 4087–4097.
[10] H.-Y. He, C.-H. Hsu, H.-Y. Chang, X.-K. Yang, P.M. Chhetri, D.M. Proserpio, J.-D. Chen, Cryst. Growth & Des. 17 (2017) 1991–1998.
[11] D. Zhang, Z.-Z. Xue, J. Pan, J.-H. Li, G.-M. Wang, Cryst. Growth & Des. 18 (2018) 1882–1890.
[12] A. Mitra, C.T. Hubley, D.K. Panda, R.J. Clark, S. Saha, Chem. Commun. 49 (2013) 6629–6631.
[13] T.R. Cook, Y.-R. Zheng, P.J. Stang, Chem. Rev. 113 (2013) 734–777.
[14] W.-D. Li, J.-L. Li, X.-Z. Guo, Z.-Y. Zhang, S.-S. Chen, Metal(II) Coordination Polymers Derived from Mixed 4-Imidazole Ligands and Carboxylates: Syntheses, Topological Structures, and Properties, in: Polymers (Basel), 2018.
[15] S. Dawn, S.R. Salpage, M.D. Smith, S.K. Sharma, L.S. Shimizu, Inorg. Chem. Commun. 15 (2012) 88–92.
[16] L.-L. Tian, C. Wang, S. Dawn, M.D. Smith, J.A. Krause, L.S. Shimizu, J. Am. Chem. Soc. 131 (2009) 17620–17629.
[17] S.R. Salpage, A. Paul, B. Som, T. Banerjee, K. Hanson, M.D. Smith, A.K. Vannucci, L.S. Shimizu, Dalton Transactions 45 (2016) 9601–9607.
[18] F. Xue, J. Fang, S.L. Delker, H. Li, P. Martásek, L.J. Roman, T.L. Poulos, R.B. Silverman, J. Med. Chem. 54 (2011) 2039–2048.
[19] Y. Imaeda, H. Tokuhara, Y. Fukase, R. Kanagawa, Y. Kajimoto, K. Kusumoto, M. Kondo, G. Snell, C.A. Behnke, T. Kuroita, ACS Med. Chem. Lett., 7 (2016) 933-938
[20] A.M. Fuller, D.A. Leigh, P.J. Lusby, I.D.H. Oswald, S. Parsons, D.B. Walker, Angew. Chem. Int. Ed. 43 (2004) 3914–3918.
[21] A.R. Mitchell, P.F. Pagoria, C.L. Coon, E.S. Jessop, J.F. Poco, C.M. Tarver, R.D. Breithaupt, G.L. Moody, Propellants, Explosives, Pyrotechnics 19 (1994) 232–239.
[22] [22] APEX3 Version 2016.5-0 and SAINT+ Version 8.38A. Bruker Nano, Inc., Madison, WI, USA, 2019.
[23] L. Krause, R. Herbst-Irmer, G.M. Sheldrick, D. Stalke, J. Appl. Crystallogr. 48 (2015) 3–10.
[24] G. Sheldrick, Acta Cryst. A 71 (2015) 3–8.
[25] G. Sheldrick, Acta Cryst. C 71 (2015) 3–8.
[26] O.V. Dolomanov, L.J. Bourhis, R.J. Gildea, J.A.K. Howard, H. Puschmann, J. Appl. Crystallogr. 42 (2009) 339–341.
[27] K. Roy, C. Wang, M.D. Smith, P.J. Pellechia, L.S. Shimizu, J. Org. Chem. 75 (2010) 5453–5460.
[28] I. Thondorf, Journal of the Chemical Society, Perkin Transactions 2 (1999) 1791–1796.
[29] V. Böhmer, Angewandte Chemie International Edition in English, 34 (1995) 713-745
[30] J. Jia, A.J. Blake, N.R. Champness, P. Hubberstey, C. Wilson, M. Schröder, Inorg. Chem. 47 (2008) 8652–8664.
[31] J. Conesa-Egea, C.D. Redondo, J.I. Martínez, C.J. Gómez-García, Ó. Castillo, F. Zamora, P. Amo-Ochoa, Inorg. Chem., 57 (2018) 7568-7577
[32] T.H. Kim, Y.W. Shin, J.H. Jung, J.S. Kim, J. Kim, Angew. Chem. Int. Ed. 47 (2008) 685–688.
[33] A. Kobayashi, M. Fujii, Y. Shigeta, M. Yoshida, M. Kato, Inorg. Chem. 58 (2019) 4456–4464.